

Optimizing BI-RADS 4 Lesion Assessment using Lightweight Convolutional Neural Network with CBAM in Contrast Enhanced Mammography

Oladosu O. Oladimeji^{1,2,3[0000-0001-8835-6156]}, Hamail Ayaz^{1,2,3[0000-0003-3407-9207]}, Ian McLoughlin^{4[0000-0003-0424-4849]}, and Saritha Unnikrishnan^{1,2,3[0000-0001-8711-2934]}

¹ Mathematical Modelling and Intelligent Systems for Health and Environment (MISHE), Faculty of Engineering and Design, Atlantic Technological University, Sligo, Ireland.

² Health and Biomedical Strategic Research Centre, Atlantic Technological University, Sligo, Ireland.

³ Center for Precision Engineering, Materials and Manufacturing Research (PEM), Faculty of Engineering and Design, Atlantic Technological university, F91 YW50, Sligo, Ireland. {S00243011,hamail.ayaz, saritha.unnikrishnan}@atu.ie

⁴ Department of Computer Science and Applied Physics, Atlantic Technological university, Galway, Ireland.
ian.mcloughlin@atu.ie

Abstract. Breast cancer is the leading cause of cancer-related mortality and morbidity among women worldwide. Early detection plays a crucial role in improving survival rates and BI-RADS classification is one of the effective ways of predicting breast cancer. However, BI-RADS Category 4 encompasses a broad spectrum of malignancy probabilities, ranging from over 2% to 95%. Due to the wide malignancy likelihood range and the ambiguous qualitative attributes of BI-RADS 4, patients are subjected to overdiagnosis and unnecessary procedures, such as biopsy, which entail a certain degree of physical trauma as well as financial strain. This study proposed a lightweight CNN where MobileNet serves as the backbone architecture, augmented with the Convolutional Block Attention Module (CBAM), resulting in the MobileNet-CBAM model. The model demonstrated good performance in discriminating BI-RADS 4 category malignant and benign cases in Contrast Enhanced Spectral Mammogram (CESM) with a prediction of 82%, 82% and 0.91 for accuracy, f1-score and roc-auc respectively. Additionally, for clinical friendliness, the model explanation was given using SHAP. Hence, the model presents potential utility in predicting breast cancer for lesions categorized as BI-RADS category 4 in breast imaging.

Keywords: Breast cancer · Breast Imaging Reporting and Data System (BI-RADS) · MobileNet · CBAM (Convolution Block Attention Module) · Contrast Enhanced Spectral Mammogram · cancer screening.

1 Introduction

Deep learning-based techniques have gained popularity recently and made significant advancements in tasks related to breast cancer diagnosis [2, 25, 26]. Hence, Deep Convolutional Neural Networks (DCNNs) have been instrumental in assisting radiologists and other practitioners with the classification of tumors as benign or malignant [19]. However, out of the seven Breast Imaging Reporting and Data System (BI-RADS) categories by the American College of Radiology (ACR) [12], the BI-RADS category 4 is often misdiagnosed. Due to the unclear qualitative attributes of the BI-RADS category 4, the malignancy rate spans widely from 2% to 95% [17]. As a result, patients are subjected to overdiagnosis and unnecessary treatment or surgical procedures, such as biopsy to affirm the status of the malignancy in microscopic view [11], which entails a certain degree of physical trauma as well as financial strain [23, 18].

Hence, few researchers have devised deep learning models utilising distinct imaging modalities and characteristics. Additionally, eXplainable AI frameworks were then used to explain the model and highlight the significant region in the medical image. Liu *et al* [9] proposed a combined deep learning model that incorporates both full-field digital mammography and clinical variables to predict malignancy in BI-RADS 4 category lesions. The clinical variables were transformed into a 512-bit vector through a fully connected layer. This vector was then concatenated with the image (mammography) feature vectors extracted from the MobileNetV2 network for the prediction. The model had an AUC of 0.910, and a sensitivity and specificity of 0.853 and 0.919, respectively. Grad-CAM was then utilized to highlight important regions in the classification and provide explanations for the model. Mao *et al* [13] utilized heavyweight networks including DenseNet-121, Xception, and ResNet-50 pre-trained architecture coupled with convolutional block attention module (CBAM) to classify breast lesions on Contrast Enhanced Spectral Mammography images (CESM). The CBAM-based Xception performed best among the three models for the BI-RADS 4 category with an AUC of 0.906 and an accuracy of 0.805. Thereafter, heatmaps were generated through Grad-CAM to highlight the most significant region in the image.

Despite these works, challenges still exist in classifying BI-RADS 4 category lesions as a result of the computational complexity of the heavyweight models or clinical information added to lightweight models which increases the number of parameters. Furthermore, Grad-CAM used for explainability is not effective enough to distinguish the tumor region. This is because Grad-CAM operates on a single convolutional layer at a time.

Similarly, this study focuses on BI-RADS category 4 due to its wide range of malignancy likelihood and ambiguous qualitative attributes, which typically lead to biopsy recommendation. Additionally, this research uses CESM which is a novel breast imaging that integrates conventional mammography with the administration of contrast medium to offer enhanced information [10]. Summarily, the major contributions of this work are highlighted as follows:

- Unlike most of the existing works that combined clinical information with imaging features or used heavy-weight models, which increases the model complexity and can cause model instability, this study uses pre trained lightweight MobileNet to extract features.
- Attention Mechanisms were used to focus on tumor relevant features thereby reducing the irrelevant features, number of training parameters, and consuming less computational time.
- Extensive empirical experimentation was conducted to elucidate model predictions, utilizing the absolute SHAP difference between image and SHAP values. Hence, providing clinical friendliness and applicability.

2 Methodology

2.1 Dataset Description and Augmentation

The Categorized Digital Database for Low Energy and Subtracted Contrast Enhanced Spectral Mammography images (CDD-CESM) by [8] sourced from the Cancer Imaging Archive [5] was used for this study. The dataset entails six BI-RADS categories with 801, 331, 189, 319, 358 and 8 for categories one to six respectively. The BI-RADS category 4 of the dataset which entails 126 (92 malignant and 34 benign) subtracted images and 193 (153 malignant, 39 benign and a normal) low-energy images was utilized. This study uses both the subtracted and low-energy images and the normal case was used as benign summing up to 319 images that entail both the Mediolateral Oblique (MLO) and Craniocaudal (CC) views. CESM was chosen because it can serve as a sensitive diagnostic tool for detecting and staging breast cancer, offering higher specificity but lower sensitivity compared to contrast-enhanced breast MRI [21]. The images were resized to 224x224 and normalized with division by 255. Basic augmentation techniques were used to address the limited dataset challenge and address overfitting concerns during the training of the model. To increase the dataset, the benign instances were rotated at 180 degrees, flipped horizontally and vertically, translated and a combination of rotation and translation. To balance the classes, the malignant instances were rotated at 180 degrees. Rotation, flipping and translation commonly used in medical imaging were applied [4]. Figure showcases instances of these augmentation techniques in the dataset. After applying these augmentation techniques, the malignant class was increased to 490 instances and the benign class to 444 instances, respectively.

2.2 MobileNet-CBAM

In this study, the MobileNet-CBAM entails MobileNet and CBAM as shown in Fig. 1., the MobileNet architecture [14] with pre-trained weights from ImageNet, was used to extract features from the CESM. To maintain the integrity of the weights in the convolutional and max-pooling layers and prevent their alteration, the decision was made to freeze them during the training process. The reason

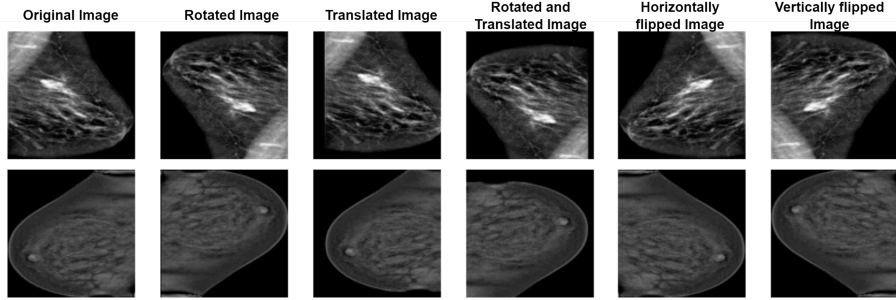


Fig. 1. The data augmentation technique visualization used in the dataset

for the choice of MobileNet is that it is a lightweight model. Hence, it effectively addresses the challenges of training small datasets and mitigates the risk of overfitting. Its efficient design optimizes memory consumption and faster processing speed compared to other convolutional neural networks (CNNs), facilitating experimentation and parameter optimization [7].

The MobileNet layers including the Convolutional and global pooling layers were used to extract the features which was passed to the CBAM block. The attention mechanism focuses on discerning the crucial features within the input image [3]. By directing the convolutional neural network (CNN) to prioritize these vital features during training, computational resources are efficiently allocated, leading to enhanced model efficiency and accuracy. The CBAM (the dashed box in Fig. 3.1) which is a lightweight attention module developed by [20] was used in this study, it comprises two sub-modules: the Channel Attention Module (blue box in Fig. 3.1) and the Spatial Attention Module (green box in Fig. 3.1). These components compute attention weights for both channel and spatial dimensions, respectively [15]. As shown in Fig. 1, the channel attention module, the feature $\mathbf{F} \in \mathbb{R}^{H \times W \times C}$, (Where C is the Channel, H is the height and W is the Width, F is the feature) obtained from the MobileNet is fed into both an average pooling layer and a maximum pooling layer. Subsequently, two shared dense layers are employed to process the input features unlike the conventional CBAM, ReLU activations were used to capture more complex channel relationships specifically non-linear interactions within the feature maps resulting in two processed channel features.

$$\mathbf{M}_{lp} = \sigma(\mathbf{W}_2 \cdot \text{ReLU}(\mathbf{W}_1 \cdot \mathbf{F}_{avg})) + \sigma(\mathbf{W}_2 \cdot \text{ReLU}(\mathbf{W}_1 \cdot \mathbf{F}_{max}))$$

where \mathbf{W} is the weights of the dense layers. Following the element-wise addition of the average and maxpooled features, the Sigmoid activation function [22] is applied to acquire the weight $\mathbf{M}_c = \sigma(\mathbf{F}_{avg} + \mathbf{F}_{max})$, and the channel attention feature is derived by multiplying the weight with the initial input feature $\mathbf{F}_c = \mathbf{M}_c \odot \mathbf{F}$. The channel feature (\mathbf{F}_c) is fed into the spatial attention module. The module operates on the feature using average pooling $\mathbf{F}_{avg}^{spatial} = \text{AvgPool}(\mathbf{F}_c)$ and max pooling layers $\mathbf{F}_{max}^{spatial} = \text{MaxPool}(\mathbf{F}_c)$. In

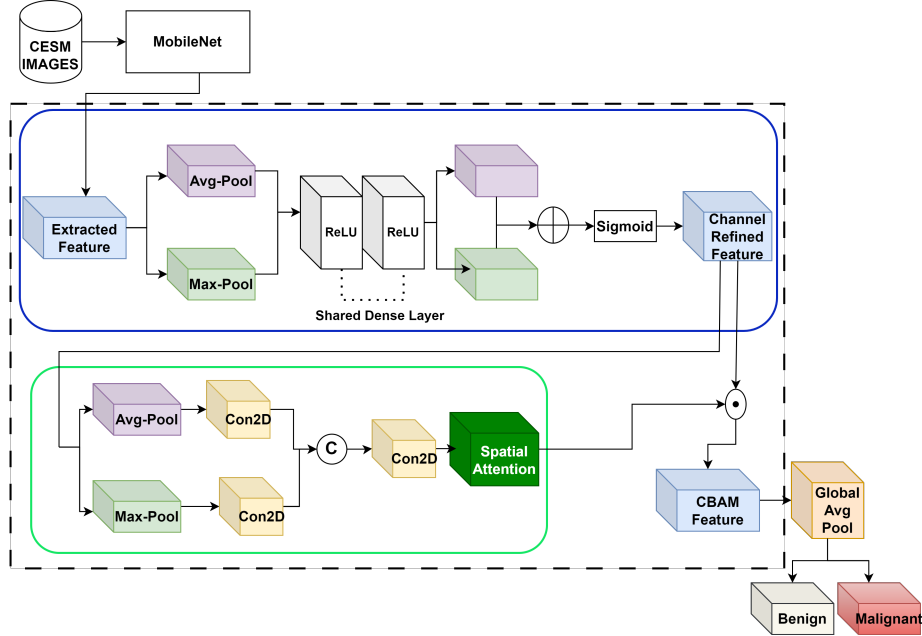


Fig. 2. The MobileNet-CBAM Architecture illustrating MobileNet for feature extraction, the integration of the Channel and Spatial Attention Mechanism.

this study, a 1×1 convolutional layer with a ReLU activation was used for each pooling to produce single-channel feature maps

$$\mathbf{M}_{avg}^{spatial} = \text{ReLU}(\mathbf{W}_3 \cdot \mathbf{F}_{avg}^{spatial}), \mathbf{M}_{max}^{spatial} = \text{ReLU}(\mathbf{W}_3 \cdot \mathbf{F}_{max}^{spatial})$$

where \mathbf{W} is the weights of the convolutional layer. These feature maps are then concatenated along the channel axis and activated using a ReLU function $\mathbf{F}_{concat} = \text{ReLU}(\text{Concat}[\mathbf{M}_{avg}^{spatial}, \mathbf{M}_{max}^{spatial}])$ unlike the originally proposed CBAM without ReLU, here ReLU is utilized in capturing non-linear relationships between the concatenated features, potentially improving the model's ability to distinguish between relevant and irrelevant spatial regions. A 1×1 convolutional layer with a sigmoid activation function is applied to the fused feature map to generate the spatial attention map $\mathbf{M}_s = \sigma(\mathbf{W} \cdot \mathbf{F}_{concat})$. The output of the CBAM module $\mathbf{F}_{out} = \mathbf{M}_s \odot \mathbf{F}_c$ is then subjected to global average pooling, which is then fed into a fully connected layer with Sigmoid activation, yielding the final output of the CBAM module.

2.3 Model Explainability

For the model explainability and clinical friendliness, SHapley Additive exPlanations (SHAP) were used to provide explainability for the model. A SHAP Gradient Explainer was instantiated using the model and the background data.

Hence, computing the SHAP values, to provide insight into the contribution and importance of each feature to the model’s predictions. Thereafter, for comparison and visualization, the SHAP values were scaled to a range between 0 and 1. To highlight discrepancies between the model’s interpretation and the actual image features, the absolute difference between the scaled SHAP values and the actual image values is computed. The absolute differences were visualized using a heatmap to highlight regions of high discrepancy between the SHAP values and the actual image. For comparison purpose, Gradient-weighted Class Activation Mapping (Grad-CAM) which was used in the existing state-of-the-art studies was also utilized for explainability. Hence, saliency maps were generated by applying Grad-CAM to the last convolutional layer of the network.

3 Experimental Results and Discussion

The algorithms utilized in this research were built upon Tensorflow 2.10.0 [16] and Keras 2.10.0, Python 3.9.16, and OpenCV, an open-source computer vision library. The computing environment is based on Windows 11 (64-bits) with Intel (R) Core(TM) I7-12850HX @ 2.10GHz. The dataset was split into 80% training and 20% testing. The training and test set entails 747 and 187 images respectively. The model was trained using five-fold cross-validation on the training set and the remaining 20% was used for independent tests. For the experiment, an Adam optimizer with a batch size of 16 and binary cross-entropy loss function was used for the parameter. The model was made to train for 40 epochs for each fold.

This section gives the results of MobileNet-CBAM performance. The evaluation of the model was based on metrics such as accuracy, precision, recall, and Area under the ROC Curve (AUC). Fig. 3.1 showcases the Receiver Operating Characteristic (ROC) curve, AUC of the training folds and the mean and standard deviation performance of the model.

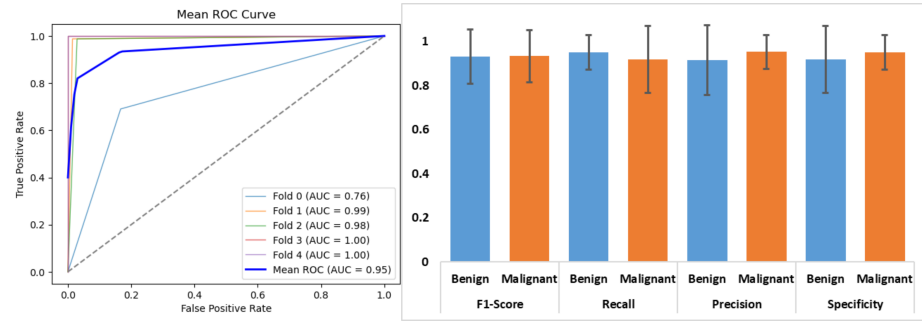


Fig. 3. The five folds training ROC Curve and Results of the MobileNet-CBAM Mean Performance.

The average performance of the model is promising and the error bars (standard deviation) are below 0.15 indicating the stability and reliability of the model. Based on the ROC curve, the true positive rate is zero when the false positive rate is zero. When the true positive rate exceeds 0.9 for the last four folds, the false positive rate reaches one. All the folds are above the diagonal line, indicating better-than-random performance.

3.1 Compared with Existing State-of-the-art Methods

This section compares the efficacy of MobileNet-CBAM against other existing methods in terms of accuracy, AUC, F1-score, precision, recall and training time in minutes. The existing methods were developed, trained and tested on the same dataset. The results of the comparison based on the testset are showcased in Table 1.

Table 1. Comparison of classification results for lightweight models.

Architecture	Accuracy	Recall	Precision	F1-score	AUC	Time (Minutes)
DenseNet-201 [1]	0.5187	0.5187	0.7597	0.3907	0.7597	241.038
EfficientNetB7 [6]	0.7326	0.7326	0.8018	0.71966	0.9059	488.927
MobileNetV2 [9]	0.5187	0.5187	0.7597	0.3907	0.7597	106.727
Xception+CBAM [13]	0.7326	0.7326	0.7378	0.7322	0.8048	197.551
Proposed	0.8235	0.8235	0.8248	0.8235	0.9149	72.347

From Table 1 . one can observe that results obtained from MobileNet-CBAM achieved superior performance compared to the existing state-of-the-art approaches including EfficientNetB7, MobileNetV2, DenseNet201 and Xception with the conventional CBAM in terms of the accuracy, precision, F1-score as well as the prediction time. MobileNet incorporates depth-wise separable convolutions to improve accuracy while maintaining efficiency by reducing the number of parameters and computational costs based on the depthwise convolutions. MobileNet-CBAM had a mean accuracy of 0.9439 and AUC of 0.9457 in the five-fold cross-validation. The experimental analysis on a separate test-set validates the performance of the MobileNet-CBAM. Figure showcases the ROC-AUC of the five-fold cross-validation of CBAM as well as the confusion matrix for the independent testset. Additionally, the training time for Mobile-CBAM is lower compared to the existing state-of-the-art approaches as they require more time for training due to their larger size and complexity, while they all have comparable testing times.

3.2 Model Interpretability

To highlight discrepancies between the model’s interpretation and the actual image features, the absolute difference between the SHAP values and the actual

image is computed. Fig 4 shows the input image with the given annotations (A), Grad-CAM (B), SHAP value visualization (C) and the absolute difference between SHAP XAI and input image (D). However, as shown in B and C, it is challenging to explain the model. Hence, the absolute difference was calculated. Based on the results of the absolute difference, the relevant tumor regions are highlighted in blue and pink while the background is in orange and other breast regions are green and yellow. For the Grad-CAM, red and yellow regions indicate areas with higher predictive significance compared to the green and blue regions. The absolute difference visualization was consistent with the lesion regions based on the annotations provided as it is able to identify the tumor homogeneity and heterogeneity. The visualizations indicate that SHAP absolute difference provided better visualization compared to Grad-CAM used in the previous works as Grad-CAM relies on the last convolutional layer while SHAP rely on the entire model layers. Therefore, providing better explainability.

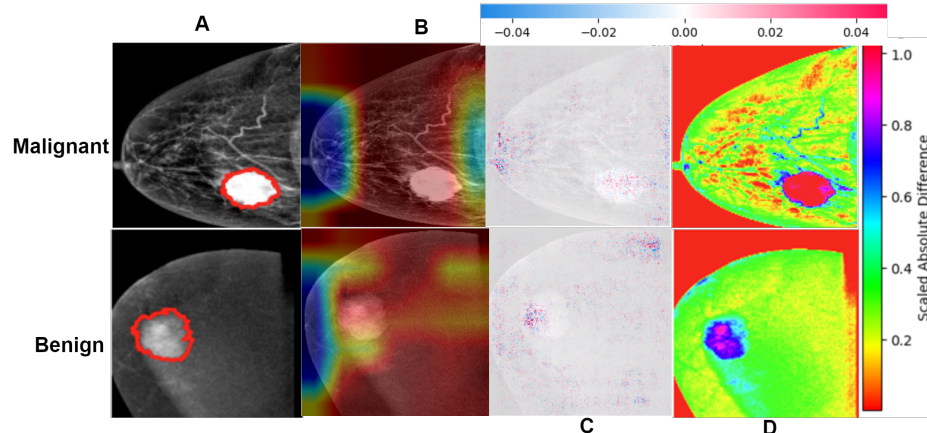


Fig. 4. The result of the Model Explainability including the annotation provided for the dataset (A), Grad-CAM (B), SHAP Value (C) and Absolute Difference (D).

This study focuses on malignancy classification in BI-RADS 4 CESM using MobileNet-CBAM. In clinical practice, patients with BI-RADS 4 category still require a biopsy to determine the malignancy which comes with several risks [24]. This study aims to reduce unnecessary biopsies without compromising diagnostic accuracy. In the clinical context, the results suggest that integrating the MobileNet-CBAM model into real-world settings could result in more accurate and timely diagnoses of BI-RADS 4 breast cancer. The experimental results indicate that the approach outperforms the existing state-of-the-art approaches including large-scale CNN DenseNet-201 [1], lightweight CNNs including EfficientNetB7 [6] and MobileNetV2 [9] and attention-based CNN Xception+CBAM [13] this further proves the superiority of the model. Despite the substantial

number of parameters of backbone models, it is overfitting due to the size of the dataset. The dataset is not large enough to justify its complexity. Additionally, the model is more generalizable as it has been trained on both CC and MLO views. This study demonstrated that the attention mechanisms of the model enable the model to selectively emphasize pertinent features while suppressing noise, thus contributing to its exceptional performance as well as reducing the training time. It would be interesting in future research to explore the combination of radiomic features with the imaging features to have a more robust model; as radiologists often utilize morphological characteristics like size, volume, and contour to evaluate breast lesions and make diagnoses [24]. One of the limitations of this study is the limited dataset, as CESM is a relatively new technology [13]; future research would evaluate the model on large data size.

4 Conclusions

Despite advancements in experience and technology, the subjective nature of BI-RADS category 4 remains a concern. Hence, this study proposed and developed a model for automatic BI-RADS category 4 malignancy prediction in CESM images. The MobileNet-CBAM model had an accuracy and AUC of 82% and 91% respectively. The model has the potential to assist, improve the efficiency and reduce the workloads of radiologists in diagnosing breast cancer. In future work, the model would be evaluated on a larger dataset to enhance the generalizability.

Acknowledgments. This research is funded by the Modelling & Computation for Health And Society (MOCHAS) Postgraduate Research Training Programme (PRTP) Scholarship, Atlantic Technological University, Ireland .

Disclosure of Interests. The authors have no competing interests to declare that are relevant to the content of this article.

References

1. Achak, A., Hedyehzadeh, M.: Determining the differentiation of benign and malignant nme lesions in contrast-enhanced spectral mammography images based on convolutional neural networks. *Journal of Medical and Biological Engineering* **43**(5), 585–595 (2023)
2. Boumaraf, S., Liu, X., Ferkous, C., Ma, X.: A new computer-aided diagnosis system with modified genetic feature selection for bi-rads classification of breast masses in mammograms. *BioMed Research International* **2020**(1), 7695207 (2020)
3. Chen, L., Yao, H., Fu, J., Ng, C.T.: The classification and localization of crack using lightweight convolutional neural network with cbam. *Engineering Structures* **275**, 115291 (2023)
4. Chlap, P., Min, H., Vandenberg, N., Dowling, J., Holloway, L., Haworth, A.: A review of medical image data augmentation techniques for deep learning applications. *Journal of Medical Imaging and Radiation Oncology* **65**(5), 545–563 (2021)

5. Clark, K., Vendt, B., Smith, K., Freymann, J., Kirby, J., Koppel, P., Moore, S., Phillips, S., Maffitt, D., Pringle, M., et al.: The cancer imaging archive (tcia): maintaining and operating a public information repository. *Journal of digital imaging* **26**, 1045–1057 (2013)
6. Helal, M., Khaled, R., Alfarghaly, O., Mokhtar, O., Elkorany, A., Fahmy, A., El Kassas, H.: Validation of artificial intelligence contrast mammography in diagnosis of breast cancer: Relationship to histopathological results. *European Journal of Radiology* p. 111392 (2024)
7. Kaya, Y., Gürsoy, E.: A mobilenet-based cnn model with a novel fine-tuning mechanism for covid-19 infection detection. *Soft Computing* **27**(9), 5521–5535 (2023)
8. Khaled, R., Helal, M., Alfarghaly, O., Mokhtar, O., Elkorany, A., El Kassas, H., Fahmy, A.: Categorized contrast enhanced mammography dataset for diagnostic and artificial intelligence research. *Scientific Data* **9**(1), 122 (2022)
9. Liu, H., Chen, Y., Zhang, Y., Wang, L., Luo, R., Wu, H., Wu, C., Zhang, H., Tan, W., Yin, H., et al.: A deep learning model integrating mammography and clinical factors facilitates the malignancy prediction of bi-rads 4 microcalcifications in breast cancer screening. *European Radiology* **31**, 5902–5912 (2021)
10. Long, R., Cao, K., Cao, M., Li, X.T., Gao, F., Zhang, F.D., Yu, Y.Z., Sun, Y.S.: Improving the diagnostic accuracy of breast bi-rads 4 microcalcification-only lesions using contrast-enhanced mammography. *Clinical Breast Cancer* **21**(3), 256–262 (2021)
11. Luo, L., Wang, X., Lin, Y., Ma, X., Tan, A., Chan, R., Vardhanabhuti, V., Chu, W.C., Cheng, K.T., Chen, H.: Deep learning in breast cancer imaging: A decade of progress and future directions. *IEEE Reviews in Biomedical Engineering* (2024)
12. Magny, S.J., Shikhman, R., Keppke, A.L.: Breast imaging reporting and data system. In: StatPearls [Internet]. StatPearls publishing (2022)
13. Mao, N., Zhang, H., Dai, Y., Li, Q., Lin, F., Gao, J., Zheng, T., Zhao, F., Xie, H., Xu, C., et al.: Attention-based deep learning for breast lesions classification on contrast enhanced spectral mammography: a multicentre study. *British journal of cancer* **128**(5), 793–804 (2023)
14. Nan, Y., Ju, J., Hua, Q., Zhang, H., Wang, B.: A-mobilenet: An approach of facial expression recognition. *Alexandria Engineering Journal* **61**(6), 4435–4444 (2022)
15. Oladimeji, O.O., Ibitoye, A.O.J.: Brain tumor classification using resnet50-convolutional block attention module. *Applied Computing and Informatics* (ahead-of-print) (2023)
16. Pang, B., Nijkamp, E., Wu, Y.N.: Deep learning with tensorflow: A review. *Journal of Educational and Behavioral Statistics* **45**(2), 227–248 (2020)
17. Spak, D.A., Plaxco, J., Santiago, L., Dryden, M., Dogan, B.: Bi-rads® fifth edition: A summary of changes. *Diagnostic and interventional imaging* **98**(3), 179–190 (2017)
18. Tang, Y., Liang, M., Tao, L., Deng, M., Li, T.: Machine learning-based diagnostic evaluation of shear-wave elastography in bi-rads category 4 breast cancer screening: a multicenter, retrospective study. *Quantitative Imaging in Medicine and Surgery* **12**(2), 1223 (2022)
19. Wang, J., Zheng, Y., Ma, J., Li, X., Wang, C., Gee, J., Wang, H., Huang, W.: Information bottleneck-based interpretable multitask network for breast cancer classification and segmentation. *Medical Image Analysis* **83**, 102687 (2023)
20. Woo, S., Park, J., Lee, J.Y., Kweon, I.S.: Cbam: Convolutional block attention module. In: Proceedings of the European conference on computer vision (ECCV). pp. 3–19 (2018)

21. Yasin, R., El Ghany, E.A.: Birads 4 breast lesions: comparison of contrast-enhanced spectral mammography and contrast-enhanced mri. *Egyptian Journal of Radiology and Nuclear Medicine* **50**, 1–10 (2019)
22. Yin, X., Goudriaan, J., Lantinga, E.A., Vos, J., Spiertz, H.J.: A flexible sigmoid function of determinate growth. *Annals of botany* **91**(3), 361–371 (2003)
23. Zhang, R., Wei, W., Li, R., Li, J., Zhou, Z., Ma, M., Zhao, R., Zhao, X.: An mri-based radiomics model for predicting the benignity and malignancy of bi-rads 4 breast lesions. *Frontiers in oncology* **11**, 733260 (2022)
24. Zhang, S., Shao, H., Li, W., Zhang, H., Lin, F., Zhang, Q., Zhang, H., Wang, Z., Gao, J., Zhang, R., et al.: Intra-and peritumoral radiomics for predicting malignant birads category 4 breast lesions on contrast-enhanced spectral mammography: a multicenter study. *European Radiology* **33**(8), 5411–5422 (2023)
25. Zhang, T., Mann, R.M.: Contrast-enhanced mammography: better with ai? *European Radiology* **34**(2), 914–916 (2024)
26. Zhang, T., Tan, T., Samperna, R., Li, Z., Gao, Y., Wang, X., Han, L., Yu, Q., Beets-Tan, R.G., Mann, R.M.: Radiomics and artificial intelligence in breast imaging: a survey. *Artificial Intelligence Review* **56**(Suppl 1), 857–892 (2023)